Origin of Efficiency Roll-Off in Colloidal Quantum-Dot Light-Emitting Diodes

Yasuhiro Shirasaki,[1] Geoffrey J. Supran,[2] William A. Tisdale,[3] and Vladimir Bulović[1]

[1]*Department of Electrical Engineering and Computer Science, Massachusetts Institute of Technology,*
Cambridge, Massachusetts 02139, USA
[2]*Department of Materials Science and Engineering, Massachusetts Institute of Technology, Cambridge, Massachusetts 02139, USA*
[3]*Department of Chemical Engineering, Massachusetts Institute of Technology, Cambridge, Massachusetts 02139, USA*
(Received 23 October 2012; revised manuscript received 26 February 2013; published 21 May 2013)

We study the origin of efficiency roll-off (also called ''efficiency droop'') in colloidal quantum-dot light-emitting diodes through the comparison of quantum-dot (QD) electroluminescence and photoluminescence. We find that an electric-field-induced decrease in QD luminescence efficiency—and not charge leakage or QD charging (Auger recombination)—is responsible for the roll-off behavior, and use the quantum confined Stark effect to accurately predict the external quantum efficiency roll-off of QD light-emitting diodes.

Quantum-dot light-emitting diodes (QD-LEDs), which capitalize on the excellent color saturation and high photoluminescence efficiency of colloidal QDs, offer the prospect of a new generation of display technologies [1]. However, these devices suffer from decreasing efficiency [measured as the ratio of the number of photons emitted out of the QD-LED to the number of electrons injected into the device, per unit time, known as external quantum efficiency (EQE)] at high current densities. This behavior, termed efficiency roll-off or efficiency droop, is a problem that affects most types of LEDs [2–4]. The origin of the efficiency roll-off continues to be a topic of debate and understanding its cause is essential to developing high-brightness, high current density QD-LEDs. In this Letter, we investigate the origins of the roll-off behavior in QD-LEDs by performing simultaneous measurements of electroluminescence (EL) and photoluminescence (PL) intensities of a QD-LED, which pinpoint the cause to be a decrease in QD luminescence efficiency. Comparison of EL and PL spectra reveals that strong electric fields are responsible for the reduced QD luminescence, and the quantum confined Stark effect (QCSE) and transient PL measurements consistently explain the observed phenomena.

The device structure investigated was a QD-LED with organic-inorganic hybrid charge transport layers that has recently attracted attention owing to its record high EQE and brightness [2]. The device was fabricated on a glass substrate coated with indium tin oxide and has the structure: ITO (150 nm)/ZnO (50 nm)/QDs (30 nm)/4, 4-bis(carbazole-9-yl) biphenyl (CBP) (100 nm)/MoO$_3$ (10 nm)/Al (100 nm). ZnO was radio-frequency sputtered, QDs were spin-cast out of chloroform, and CBP, MoO$_3$, and Al were thermally evaporated. We used CdSe-ZnCdS core-shell QDs with a peak PL wavelength of 610 nm, provided by QD Vision, Inc. Current density and normalized EQE for a typical device are shown in Fig. 1(a). The EQE peaks at 2% for

4 V applied bias and rolls-off by 50% by 8 V. The energy band diagram of the device is shown in the inset and is based on literature values [4–7].

The decrease in EQE at high biases may be a result of either charge carriers leaking out of the QD layer or a reduction in QD luminescence efficiency. To identify which of these two mechanisms dominates, we perform a simultaneous EL-PL experiment and monitor the relative PL efficiency of the QDs as the device bias is swept. To isolate the PL contribution from total luminescence, we modulate the PL excitation source ($\lambda = 530$ nm LED) at 1 kHz and send the combined EL-PL signal (collected using a Si photodiode and a current preamplifier) to a lock-in amplifier. The PL intensity is intentionally kept low (PL/EL < 0.001% at 13 V) to avoid significantly increasing the charge density within the QD layer. An excitation wavelength of 530 nm ensures that the QD layer is excited without exciting the surrounding wider band gap charge transport layers. The results of this experiment are shown in Fig. 1(b) with EQE and QD PL intensity normalized at 4 V applied bias. Below 4 V, the PL intensity remains constant (voltage independent). In contrast, above 4 V, the PL intensity decreases monotonically with increasing bias, tracking the decrease in EQE of the QD-LED. The correspondence between the decreasing PL intensities and EQE with applied bias identifies the change in the QD luminescence efficiency to be sufficient to explain the QD-LED roll-off behavior.

Reduction of PL efficiency in QD thin films has been previously measured when QDs are heated [8], charged (Auger recombination) [9], or placed under a strong electric field [10,11]. We eliminate temperature effects on the QD PL efficiency, as measurement of the operating temperature of our QD-LEDs with an infrared camera shows a change of no more than a few degrees, which is not sufficient to affect the PL efficiency and explain the roll-off. We similarly eliminate charging effects since QDs
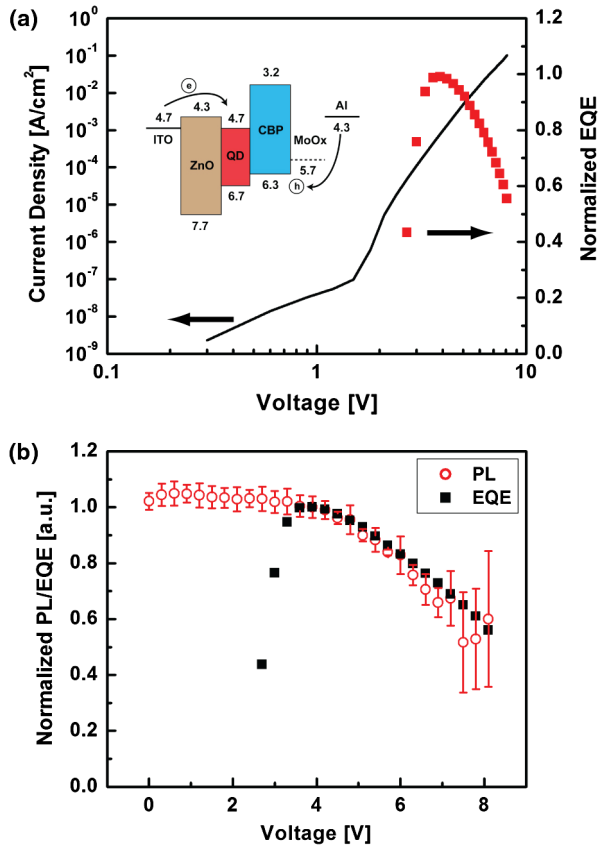
FIG. 1 (color online). (a) Current density-voltage and EQE-voltage characteristics of the QD-LED under investigation. Inset: Energy band diagram of the device, with indicated energy values referenced to the vacuum level. (b) EQE and QD PL intensity of the QD-LED (normalized at 4 V, when the peak EQE = 2%) as a function of voltage. Roll-off of the EQE above 4 V reflects reduced QD PL efficiency at high biases.

generally have a long charge retention time (on the order of minutes to hours [9]) whereas the efficiency roll-off curve [Fig. 1(b)] is measured within seconds and was repeated many times with the peak EQE unchanged. From these observations, we hypothesize that the electric field associated with the applied bias is quenching the QD luminescence at high voltages.

Earlier studies of the electric-field effect on QDs, also known as the QCSE, showed that the luminescence intensities and spectral shifts of QDs are field dependent [12]. To characterize the QCSE in our QD-LED structure, we first measured the PL spectra of the QD films in our devices under reverse bias. Reverse biasing allows the effect of electric field on the QDs in the QD-LED to be studied *in situ*, in absence of any charge injection. To avoid damaging the device by prolonged reverse biasing, we apply sawtoothlike voltage waveforms [Fig. 2(a)] with a 500 Hz repetition rate. The sawtooth amplitude peaks at −18 V and is followed by a duration of positive voltage (1.6 V) to reduce stress on the device by minimizing the average net applied voltage, but without turning on the EL.

QD PL is induced by a $\lambda = 530$ nm LED emitting 100 μs long pulses synchronized with the voltage waveform and QD PL spectra are collected with a spectrometer. By sweeping the time delay (phase shift) between the voltage waveform and the illumination pulse, PL spectra of the QDs under different electric-field strengths can be collected while keeping all other conditions unchanged. To assess the degree to which the QCSE occurs while the QD-LED is in operation, EL spectra are monitored as the device is forward biased, again with all other experimental variables held constant. This combined approach allows the study of QD PL and EL from the same active device structure.

The resulting PL and EL spectra are normalized and their peak emission energies are compared. Figure 2(b) shows EL spectra obtained at 5, 11.6, and 13.8 V overlaid with PL spectra with coincident peak energies (PL at 1.6, −8.6, and −16 V, respectively). Both PL and EL spectra are approximately Gaussians at low biases and redshift at higher biases. However, EL does not exhibit the same spectral broadening that is observed in the PL. In particular, a shoulder begins to appear on the low energy side of the PL spectra. The inset of each panel in Fig. 2(b) shows a double-Gaussian fit to each asymmetrically broadened PL spectrum. We attribute the double-Gaussian profile to emission from QD subpopulations that are subject to two different environments; for example, a layer of QDs next to ZnO and a layer of QDs away from ZnO. QDs placed adjacent to the ZnO are expected to exhibit energy levels that differ from that of QDs placed adjacent to the CBP, which has a lower dielectric constant [13]. The difference between EL and PL spectra (even when the peaks are matched) can be explained by the fact that the electric-field distribution is generally different between forward and reverse biased diodes [14], thus affecting the two populations differently.

Each PL and EL spectrum is decomposed into two Gaussians, and their intensities and peak energies as a function of device voltage are shown in Figs. 2(c) and 2(d), respectively. The black solid line in Fig. 2(c) is a fit to the PL intensity data assuming a simplified version of the model described in Ref. [10]. In Fig. 2(d), PL and EL peak energies for both subpopulations redshift under high bias. In particular, the PL peaks of subpopulation A show a quadratic dependence on voltage (black fit), which is a signature of the QCSE. There is no clear fit for the EL peak shift because the distribution of the electric field inside the diode is voltage dependent. The peak energies are maximum when the device is slightly forward biased, indicating the presence of a built-in electric field, which is expected in a diode structure.

Assuming that the EQE of the QD-LED is predominantly governed by the QCSE at high forward biases, we should be able to predict the EQE by comparing the forward-bias EL to the reverse-bias PL from
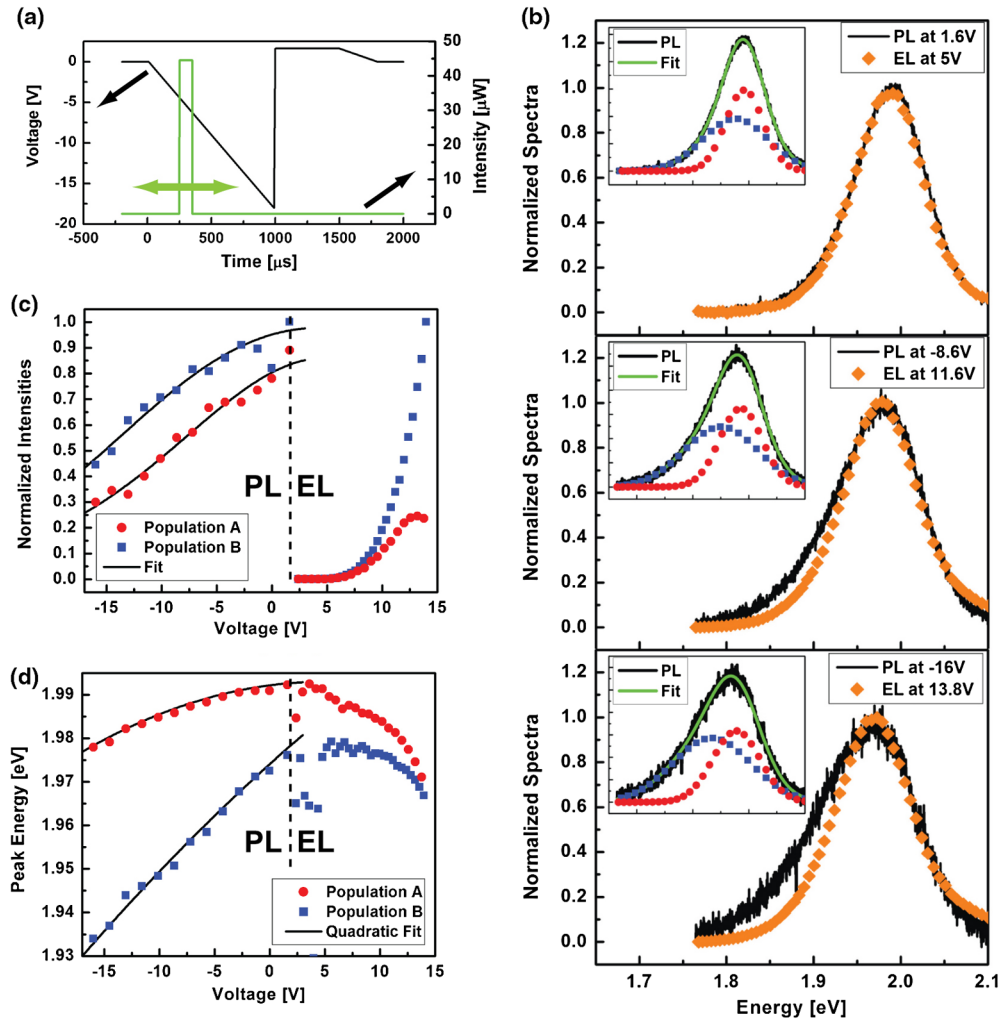
FIG. 2 (color online).   (a) Electric-field-dependent QD PL was measured by applying a sawtoothlike voltage waveform to the QD-LED and illuminating it with a 530 nm LED pulse synchronized with the voltage waveform. QD PL at varying electric fields was measured by sweeping the delay (phase) between the voltage waveform (black line) and the LED pulse (green line). (b) Comparison of QD PL spectra (black lines) and QD EL spectra (orange diamonds) at corresponding peak emission energies, for three different biases. At high biases, the PL spectrum exhibits a red shoulder that is not observed at lower biases or in the EL spectrum. Insets: PL spectra (black) are reconstructed (green) using two Gaussians, which correspond to emission from two QD subpopulations A and B (red and blue, respectively). (c) Relative intensities of subpopulations A (red) and B (blue). The PL data are fitted to a simplified version of the model presented in Ref. [10]. (d) Peak energies of subpopulation A (red) and subpopulation B (blue). Quadratic fits (black lines) to the PL data are made assuming that the shifts are due to the quantum confined Stark effect.

Figs. 2(c) and 2(d). A QD film exposed to an electric field will undergo a QCSE, which is manifested as a shift in the QD PL or EL emission spectra and a concomitant decrease in its PL or EL efficiency. Because the emission spectrum is a function of the applied field, whenever the forward-bias QD EL emission spectrum of subpopulation A (subpopulation B) matches the reverse-bias QD PL spectrum of the same subpopulation, the QDs in subpopulation A (subpopulation B) are experiencing the same local electric field under those particular EL and PL biasing conditions. Therefore, for each subpopulation, the EL efficiency at each forward bias can be predicted by finding the corresponding PL spectrum in reverse bias with peak energy matching that of the EL peak, and assigning the PL

efficiency at that electric field to the EL efficiency. We emphasize that the choice of physical model used to fit the data in Fig. 2(c) does not affect the predicted EQE, which is calculated directly from the PL and EL spectra and the corresponding PL intensities.

For example, subpopulation A [Fig. 2(d), red] shows an EL peak shift from 1.990 to 1.984 eV between 5 and 10 V. This shift corresponds to a PL peak shift from -4.5 to -11.3 V and indicates that the luminous efficiency is reduced by about 37% [Fig. 2(c)] for subpopulation A as a result of the QCSE. The relative number of excitons formed on the two subpopulations (A and B) of QDs is calculated by dividing their EL intensities in Fig. 2(c) by their respective PL efficiencies. The overall EQE is then
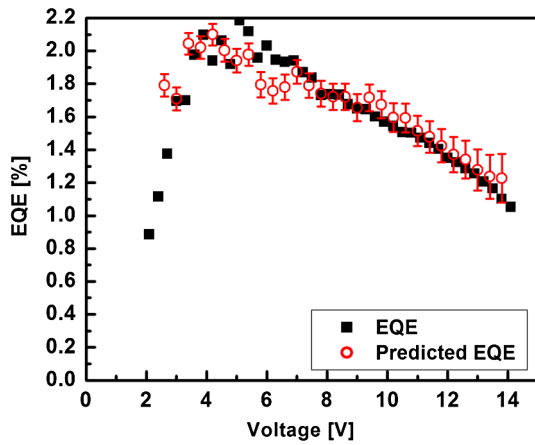
FIG. 3 (color online). Measured EQE and predicted EQE as a function of voltage. EQE is predicted through the comparison of PL and EL data [Figs. 2(c) and 2(d)] as described in the text. The agreement between the data and the prediction shows that the quantum confined Stark effect can self-consistently account for the QD-LED efficiency roll-off.

FIG. 4 (color online). Transient PL of QDs in the QD-LED reverse biased at 0, -8, -12, and -16 V. Time constants of the decays (inset) are independent of the applied voltage, suggesting that the nonradiative exciton recombination rate is independent of the electric field.

the weighted average of the PL efficiencies of the two subpopulations. This analysis is applied to EL data between 2.5 and 14 V and the resulting predicted EQE, which is scaled to match the maximum of the measured EQE, is shown in Fig. 3. Predicted and measured EQEs are in good agreement, with EQE rolling off by up to 40% at 13 V. The match between the EQE behavior predicted by the QCSE and the experimentally observed efficiency roll-off is evidence that the electric-field strength alone—and not carrier leakage or QD charging (Auger recombination)—is sufficient to model the efficiency roll-off.

To further understand the effect of the electric field on the QD PL efficiency, we measured transient PL of the QDs in the QD-LED. The same reverse biasing scheme as Fig. 2(a) was used with 100 ps laser pulse train at $\lambda = 540$ nm replacing the green excitation LED. PL was detected with a Si avalanche photodiode and timing information was obtained via a time-correlated single photon counting module. The resulting transient PL at four different voltages reveals a lifetime of 4 ns for all of the voltages applied while the initial intensity decreases with higher applied voltage (Fig. 4). The inset indicates the times at which the QD PL intensity I has decreased from its initial value of I_0 so that $I/I_0 = e^{-1}$ and $I/I_0 = e^{-2}$ ($\tau_{e^{-1}}$ and $\tau_{e^{-2}}$, respectively). Reduction of QD PL efficiency has previously been attributed to a decrease in radiative exciton recombination rate (e.g., reduced electron-hole wave function overlap [15,16]), an increase in nonradiative exciton recombination rate (e.g., exciton dissociation [17,18]), or a decrease in the probability of forming thermalized excitons (e.g., hot charge carrier trapping by QD surface traps [19,20]). Because our QD film is 8% PL efficient, PL lifetime is dominated by the nonradiative rate. Therefore, the voltage independent PL lifetime observed suggests that
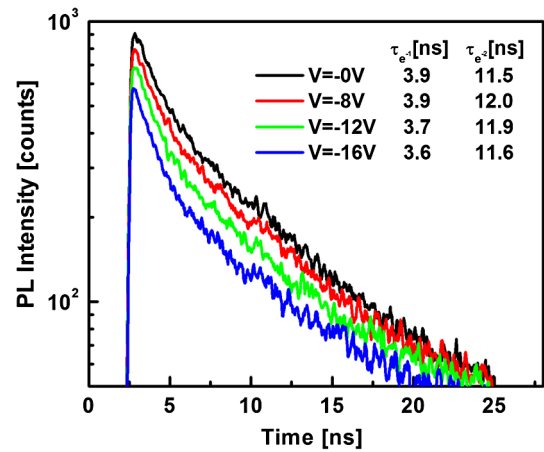
the cause is either a decrease in the radiative rate or a decrease in the thermalized-exciton formation efficiency.

In conclusion, we have identified the electric-field-induced PL quenching of QDs to be responsible for the efficiency roll-off in QD-LEDs. We use the relationship between PL peak shifts and PL quenching of QDs subject to the QCSE—observed while reverse biasing a QD-LED—to predict the efficiency roll-off in forward bias. The roll-off predicted by this analysis is in excellent agreement with our experimental data and correctly traces an EQE reduction of nearly 50%. Transient PL measurements tentatively suggest that the reduced QD luminescence efficiency is not the result of an increased nonradiative recombination rate. This is the first study offering detailed insights into the efficiency roll-off in QD-LEDs, a must for designing high-brightness QD-LEDs.

[1] Y. Shirasaki, G. J. Supran, M. G. Bawendi, and V. Bulović, Nat. Photonics **7**, 13 (2013).

[2] J. Kwak, W. K. Bae, D. Lee, I. Park, J. Lim, M. Park, H. Cho, H. Woo, D. Y. Yoon, K. Char, S. Lee, and C. Lee, Nano Lett. **12**, 2362 (2012).

[3] N. F. Gardner, G. O. Müller, Y. C. Shen, G. Chen, S. Watanabe, W. Gtz, and M. R. Krames, Appl. Phys. Lett. **91**, 243506 (2007).

[4] M. A. Baldo, S. Lamansky, P. E. Burrows, M. E. Thompson, and S. R. Forrest, Appl. Phys. Lett. **75**, 4 (1999).

[5] P. R. Brown, R. R. Lunt, N. Zhao, T. P. Osedach, D. D. Wanger, L.-Y. Chang, M. G. Bawendi, and V. Bulović, Nano Lett. **11**, 2955 (2011).

[6] P. O. Anikeeva, J. E. Halpert, M. G. Bawendi, and V. Bulović, Nano Lett. **9**, 2532 (2009).

[7] T.-H. Kim, K.-S. Cho, E. K. Lee, S. J. Lee, J. Chae, J. W. Kim, D. H. Kim, J.-Y. Kwon, G. Amaratunga, S. Y. Lee, B. L. Choi, Y. Kuk, J. M. Kim, and K. Kim, Nat. Photonics **5**, 176 (2011).

[8] D. Pugh-Thomas, B. M. Walsh, and M. C. Gupta, Nanotechnology **22**, 185503 (2011).

[9] W.-K. Woo, K. T. Shimizu, M. V. Jarosz, R. G. Neuhauser, C. A. Leatherdale, M. A. Rubner, and M. G. Bawendi, Adv. Mater. **14**, 1068 (2002).

[10] S.-J. Park, S. Link, W. L. Miller, A. Gesquiere, and P. F. Barbara, Chem. Phys. **341**, 169 (2007).

[11] H. Huang, A. Dorn, G. P. Nair, V. Bulović, and M. G. Bawendi, Nano Lett. **7**, 3781 (2007).

[12] S. A. Empedocles and M. G. Bawendi, Science **278**, 2114 (1997).

[13] C. A. Leatherdale and M. G. Bawendi, Phys. Rev. B **63**, 165315 (2001).

[14] I. H. Campbell, M. D. Joswick, and I. D. Parker, Appl. Phys. Lett. **67**, 3171 (1995).

[15] A. S. Dissanayake, J. Y. Lin, and H. X. Jiang, Phys. Rev. B **51**, 5457 (1995).

[16] G. W. Wen, J. Y. Lin, H. X. Jiang, and Z. Chen, Phys. Rev. B **52**, 5913 (1995).

[17] C. A. Leatherdale, C. R. Kagan, N. Y. Morgan, S. A. Empedocles, M. A. Kastner, and M. G. Bawendi, Phys. Rev. B **62**, 2669 (2000).

[18] M. V. Jarosz, V. J. Porter, B. R. Fisher, M. A. Kastner, and M. G. Bawendi, Phys. Rev. B **70**, 195327 (2004).

[19] C. Galland, Y. Ghosh, A. Steinbrück, M. Sykora, J. A. Hollingsworth, V. I. Klimov, and H. Htoon, Nature (London) **479**, 203 (2011).

[20] A. Pandey and P. Guyot-Sionnest, J. Phys. Chem. Lett. **1**, 45 (2010).